

This article was downloaded by:

On: 21 January 2011

Access details: *Access Details: Free Access*

Publisher *Taylor & Francis*

Informa Ltd Registered in England and Wales Registered Number: 1072954 Registered office: Mortimer House, 37-41 Mortimer Street, London W1T 3JH, UK



## The Journal of Adhesion

Publication details, including instructions for authors and subscription information:

<http://www.informaworld.com/smpp/title~content=t713453635>

### Influence of Re-adhesion on the Wear and Friction of Glass Fibre-Reinforced Polyester Composites

J. Quintelier<sup>a</sup>; P. Samyn<sup>a</sup>; P. De Baets<sup>a</sup>; L. De Doncker<sup>b</sup>; D. Van Hemelrijck<sup>c</sup>; H. Sol<sup>c</sup>

<sup>a</sup> Laboratory Soete, Ghent University, Ghent, Belgium <sup>b</sup> Hydraulics Laboratory, Ghent University, Ghent, Belgium <sup>c</sup> Department of Mechanics of Materials and Constructions, Free University Brussels, Brussels, Belgium

**To cite this Article** Quintelier, J. , Samyn, P. , De Baets, P. , De Doncker, L. , Van Hemelrijck, D. and Sol, H.(2006) 'Influence of Re-adhesion on the Wear and Friction of Glass Fibre-Reinforced Polyester Composites', *The Journal of Adhesion*, 82: 11, 1033 – 1060

**To link to this Article:** DOI: 10.1080/00218460600948453

**URL:** <http://dx.doi.org/10.1080/00218460600948453>

PLEASE SCROLL DOWN FOR ARTICLE

Full terms and conditions of use: <http://www.informaworld.com/terms-and-conditions-of-access.pdf>

This article may be used for research, teaching and private study purposes. Any substantial or systematic reproduction, re-distribution, re-selling, loan or sub-licensing, systematic supply or distribution in any form to anyone is expressly forbidden.

The publisher does not give any warranty express or implied or make any representation that the contents will be complete or accurate or up to date. The accuracy of any instructions, formulae and drug doses should be independently verified with primary sources. The publisher shall not be liable for any loss, actions, claims, proceedings, demand or costs or damages whatsoever or howsoever caused arising directly or indirectly in connection with or arising out of the use of this material.

## **Influence of Re-adhesion on the Wear and Friction of Glass Fibre–Reinforced Polyester Composites**

**J. Quintelier**

**P. Samyn**

**P. De Baets**

Laboratory Soete, Ghent University, Ghent, Belgium

**L. De Doncker**

Hydraulics Laboratory, Ghent University, Ghent, Belgium

**D. Van Hemelrijck**

**H. Sol**

Department of Mechanics of Materials and Constructions,  
Free University Brussels, Brussels, Belgium

*Based on the well-known pin-on-disc test rig, a new test setup for online measuring of wear and friction behaviour of polymer matrix composites has been developed. In contrast to a traditional friction-and-wear test rig, a steel pin and composite disc are used for studying the influence of wear debris and fibre orientation. During sliding, a thin adhesive film is possibly formed on the wear track of a composite disc, consisting of wear debris that is squeezed under the steel pin and that finally smoothens onto the composite surface. By optical microscopy, it was observed that most of the debris particles originate from the edges of the wear track. The thin film deforms continuously, with large and dark wear particles observed at the edge of the wear track. A lower coefficient of friction is achieved when the particles are re-adhered to the mating surface. The film formation mechanism depends on the normal force, sliding velocity, and bulk composite structure: because pultruded composite profiles are presently used with a layered structure, a change in film properties is observed depending on the wear depth.*

**Keywords:** Friction; Polymer composites; Re-adhesion; Wear

Received 17 May 2005; in final form 9 June 2006.

Presented in part at the 28th Annual Meeting of the Adhesion Society, Inc., in Mobile, Alabama, USA, 13–16 February 2005.

Address correspondence to Jan Quintelier, Laboratory Soete, Ghent University, St. Pietersnieuwstraat 41, Ghent 9000, Belgium. E-mail: jan.quintelier@ugent.be

## 1. INTRODUCTION

The study of polymer wear in general and polymer-based systems in particular is finding increasing citations in the literature [1] because of the availability of a wider choice of materials, ease of manufacturing, good strength, and light weight. An area where their use has been found to be very effective is the situation involving sliding contact wear [2]. Polymers are preferred in recent years over metal-based counterparts because of their low coefficients of friction [3], although their load-sustaining capacity is limited. These good sliding characteristics and the need for functioning in high-loaded tribosystems has given an impetus for industrial application of polymer composite materials (*e.g.*, in the production of bearing components used in automobile industries [4], such as gears, cams, wheels, etc.).

However, the incorporation of composite components in actual service requires good understanding of the processing-related structure and its influence on wear and friction properties. For examples, fibres with a perpendicular orientation to the sliding direction yield higher friction, whereas parallel fibre orientation results in the lowest friction [5]. A number of studies on polymer matrix composites subjected to sliding and abrasive wear indicate that wear resistance strongly depends on the intrinsic properties of the material, as well as on the external wear conditions such as applied pressure and contact velocity [4]. Well-known wear mechanisms for composites include fibre-matrix debonding, fibre cracking, and fibre pullout [6], which may vary with fibre orientation. The effects of carbon fibre orientation and surface temperatures on friction and wear of unidirectional fibre composites were investigated in detail by Tripathy and Furey [7]. Lu and Friedrich [8,9] systematically studied the influence of carbon-fibre volume fraction on friction and wear and declared that an optimum range for short carbon fibre in a PEEK matrix is between 15 to 25 vol%, according to lower specific wear rates. This reduction in wear is mainly attributed to improved load-carrying capacity, higher creep resistance, and better thermal conductivity of the fibres. However, it is known from others [10] that the addition of fibres to a bulk polymer does not necessarily improves its wear resistance. Extremely high loads make the materials sensitive to fibre fracture and fibre pulverization, whereas incorporation of fibre debris into the third-body interface favours abrasive wear [11,12]. At present, relationships between formulation and performance of polymer matrix composite materials are not clear, and complex problems involving instabilities in the coefficient of friction, excessive wear, vibration, and noise accompany the friction processes [13].

The formation of a transfer film in pure polymer sliding has been widely demonstrated as a result of high load, combined with reasonable sliding velocity. Favourable thin transfer requires a certain range of counterface roughness [14]. Also, for composites, friction processes are accompanied by the production of wear debris adhering to the rubbing couple [15–18]. A characteristic friction layer then forms on the surface, determining the sliding performance [18]. The thickness and plastification of these films play an important role in tribology [19] and cause a variation in friction and wear behaviour with time due to changes at the interface. Such tribologically induced processes have been variously described for both polymers and composites [20,21], whereas transfer also occurs for sliding of ceramics [22]. In metal sliding and brake material compositions [25], the formation of mechanically alloyed layers [23] or oxide glazes [24] was reported. The ubiquity of interfacial phenomena has led to the recognition of the critical role of third-body wear debris in determining the friction and wear behaviour of most tribosystems involving repetitive mutual sliding [26–28].

The extent of third-body debris trapping and retention is greatly affected by the contact situation, in particular geometrical parameters (*e.g.*, the tribocomponent shape or contact overlap ratio) and dynamic parameters (*e.g.*, type of motion or vibration) [28]. In a strict sense, either a transfer layer develops on the sliding counterface or a thin film grows on the wear material. The sequence of events that leads to transfer or film formation, however, includes identical processes [26–28], respectively, (i) particle detachment from the component materials, (ii) debris-particle trapping, (iii) load bearing and flow in the interface, and (iv) permanent elimination from the system as wear debris.

An in-depth analysis of the friction transfer makes it possible to identify the basic leading elements involved in this process. This process can be represented schematically in the zone of a single contact spot by the following sequence of events: contact, adhesive interaction, shear of the surface layer, repeated plastic deformation, separation of particles of the material with lower cohesive energy density, fatigue damage, dispersion, and removal from the friction zone [29]. This process (or its individual elements) usually has a cyclic nature. This scheme is obviously largely idealized, because many of the process elements are concurrent in time. Part of the material separated from the surface is always in a free or mobile state, part of the material may be in the molten and severely damaged state (temperature contributes to higher wear-particle adhesion and the formation of a monolithic film [30]), the construction of the assembly may limit removal of the material

from the friction zone, *etc.* Nevertheless, the basic elements of the process take place in all cases of friction transfer, as we demonstrate.

The compatibility of the sliding pair (material composition, compatibility, hardness, and chemical activity) or surface conditions (roughness, way of mechanical processing, surface energy) strongly influences the wear-particle movability and adhesion to one of the contact bodies. Also, the test conditions may alter the transfer ability. When the sliding velocity is decreased, the coefficient of friction increases because the transfer film cools. On the other hand, solidification of the transfer film possibly induces a decrease in friction coefficient. When the speed increases, the value of the coefficient of friction (COF) increases, which is characteristic of the solid-state film [14].

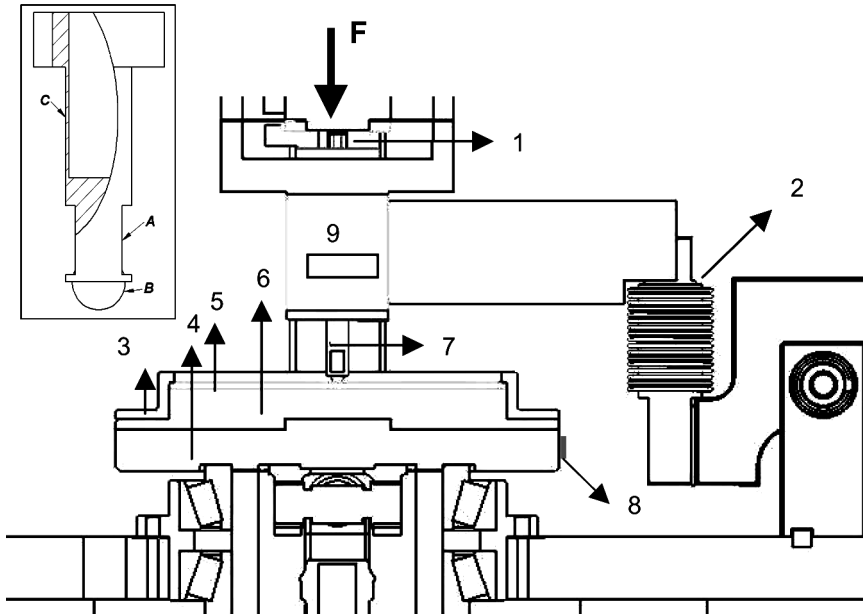
Keeping these aspects in mind, the response to dry sliding wear of glass fibre-reinforced pultruded polyester is not clearly predictable and should be further examined. Therefore, a new test setup was developed for monitoring the wear processes of pultruded composite discs, depending on material composition and test parameters. By choosing specific contact geometries, the roles of wear-debris motion and adhesion can be investigated. After wear runs, the composite wear surface and steel-pin counterface are examined using scanning electron microscope (SEM) [31] and optical microscopy. Cross-sections of the resulting wear track are studied to explain a variation of friction and wear properties with wear depth of pultruded fibre composites.

## 2. EXPERIMENTAL

### 2.1. Test Rig

A new pin-on-disc test rig (Fig. 1) was built for monitoring the tribological behaviour of composite materials as bearing material [32]. The materials, seen on most common pin-on-disc test setups cited in the literature [33–36] and which consist of a stationary composite pin in contact with a rotating steel disc, were reversed, and a composite disc and steel pin were used. This yields possibilities for investigating the influence on wear and friction response of the fibre orientation and wear debris. This wear debris accumulates in the wear track during one single test run by use of an unidirectional fibre-reinforced composite. The present test rig is valid for testing in a velocity range from 10 to 100 mm/s applied to the composite disc and a maximum normal load applied to the pin of up to 1,000 N.

The stationary pin (Fig. 1, A 7) is made of steel and has a length of 35 mm. It is hollow at the top (see inset, Fig. 1, A), because measuring the bending of the pin with strain gauges requires a sufficient strain in



**FIGURE 1** Pin-on-disc test rig, with (1) normal load cell, (2) friction load cell, (3) ring for keeping the composite disc fixed and in the centre, (4) fixed disc on the test rig, (5) composite disc, (6) removable disc where the composite test specimen is glued on, (7) pin, (8) magnets for triggering, and (9) contactless proximator counter face [32]. Inset: pin construction, with (A) positions for additional sensors, (B) the ball of the deep groove ball bearing, and (C) hollow-top construction.

the steel pin. Two flat parallel faces close to the contacting surface are used for mounting an accelerometer (see inset Fig. 1, A) and an acoustic emission sensor. Thermocouples can be placed over the entire pin geometry. A ball from a deep-groove ball bearing is used as mating surface and forms the top of the pin. So, the pin can be reused, and only the ball contact part has to be replaced.

The rotating composite disc (5) is fixed on a steel disc (6) with beeswax. High frictional forces are expected, and probably this will not prevent rotation of the disc relative to the steel disc. Therefore, the disc is additionally kept in place by an external ring (3). This ring not only presses the composite disc slightly onto the steel disc but also assures that the composite disc remains centred during the rotation with a perfectly circular wear pattern on the disc. This replaceable disc construction is placed on a fixed disc (4). The whole disc construction rests on two axial bearings and is driven by the axis

of a reduction unit, which itself is driven by an asynchronous motor through a speed reducer and timing belt.

The depth of the wear track is measured online by a contactless proximitor (9), providing an estimation of the evolution of the wear depth in time.

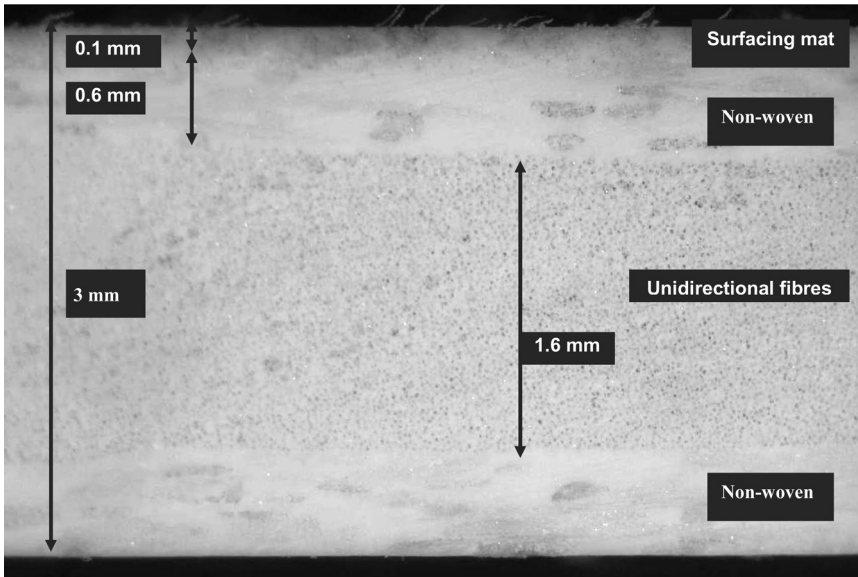
For measuring the normal force on the pin, a load cell is placed on top of the pin (1). This load cell is protected by a spring mechanism, which allows direct pressing on the load cell without damaging it. Another method to measure the normal force on the pin is by measuring the air pressure in the cylinder used as supplier for the normal force. This cylinder is connected by valves to the compressor. The friction force is measured with a load cell (2) based on bending.

Magnets (8) are placed on the rotating composite disc. They are used as a trigger for the various signals. They are also used to synchronize measured friction and wear signals with fibre orientation, as one trigger is representative for the perpendicular direction. This type of indication allows calculation of the values of the friction force related to a specific fibre orientation ( $0^\circ$ ,  $90^\circ$ ,  $180^\circ$ ,  $270^\circ$ ).

## 2.2. Test Material

The wear material used in this investigation was a pultruded composite profile of flame-retardant low-profile polyester without halogens as a matrix, reinforced with glass fibres ( $50 \pm 5$  w%) [37–41] (Exel Composites NV, Oudenaarde, Belgium). A cross-section of the structure of this material can be seen in Fig. 2. This material consists of several layers, with a nonwoven at the top and bottom (B, D) of the profile and unidirectional glass fibres in the centre (C). The region indicated with (A) is a surface mat, used for process and technical reasons. This mat contains short polyester fibres. The total thickness of this profile is 3 mm, with a central section of 1.6 mm. Mechanical properties of the material are given in Table 1. The composite specimen geometry [37] consists of discs with a fixed diameter of 160 mm. They were cut from the pultruded profiles by water jet to avoid any thermal influence. A unique fibre direction was indicated on the discs before cutting. Because all samples were taken from one single pultruded profile, the quality of the specimens is constant.

The contact surface is a ball-bearing steel grade (hardness 63 HRC, composition: C = 1.03%, Si = 0.25%, Mn = 0.35%, Cr = 1.4%). It has a diameter of 8 mm within narrow tolerances and constant roughness, and it was fixed into the pin with a two-component adhesive. No rotation of this ball in the pin is ever seen during testing, indicating good adhesion of ball in the pin.



**FIGURE 2** Cross-section of the composite material, with a surface mat, two nonwovens, and a bulk zone with unidirectional fibres.

### 2.3. Test Parameters

The test program is based on different combinations of load and speed, resulting in various PV values, an important mechanical parameter for the use and characterization of these materials in bearing applications. The PV value is the product of the applied load and speed. The value limiting the severe wear conditions gives an expression of the bearing capacity of this material. It is important to note that this value is determined by, and correlated to, a certain allowable wear rate [36].

**TABLE 1** Properties of the Pultruded Plates

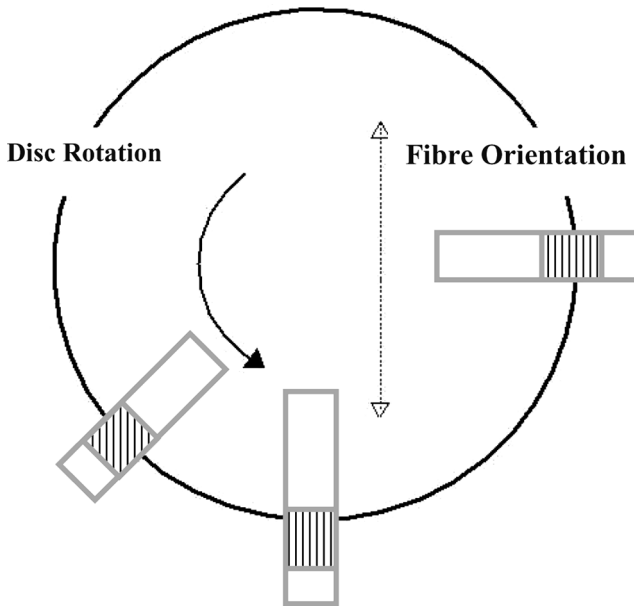
Parameter	Unit	Glass fibre-reinforced polyester
Typical glass content	vol. %	50 ± 5%
Tensile strength	GPa	1.0–1.2
Tensile modulus	MPa	42–45
Flexural strength	MPa	1000–1300
Flexural modulus	MPa	40–43
Coefficient of thermal expansion	10 <sup>-6</sup> /K	6–8
Density	kg/dm <sup>3</sup>	1.9–2.0



The friction force is defined as the force needed to overcome adhesion and to keep both materials (steel pin and composite disc) in relative motion. If this force is divided by the applied normal force, the coefficient of friction (COF) is obtained. This coefficient is a value for the ease of motion between both materials. In this investigation, only the kinetic friction force is measured. The static friction force, which is the minimum force needed to get both samples in relative motion starting from an initial zero relative speed, is not measured in present dynamic testing, because no start–stop conditions occur during constant rotation.




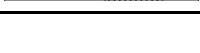
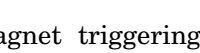
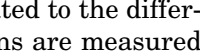
Tests are performed at a constant room temperature of 20°C, with a sliding speed at the centre of the wear track varying from 10 mm/s to 40 mm/s and a normal load varying from 60 N to 300 N. Tests run for 10,000 rounds of 400 mm each (the diameter of the wear track is chosen at 127 mm), yielding a total sliding distance for the pin of 4 km. The total sliding time for each test varies from 100,000 s (40 mm/s) to 400,000 s (10 mm/s). The time for one single rotation varies from 10 s to 40 s.

Friction coefficients and wear depths are continuously measured over the full disc rotation. In the following graphs, which present friction and wear as a function of the total sliding time, values are



**FIGURE 3** Scheme for cutting out the test specimens for further SEM research.

**TABLE 2** Numbering and Properties of Test Samples for SEM

Sample number	Fibre orientation related to the direction of movement	Treatment	Fibre orientation
M1	90°	Original	
M3	90°	Cleaned	
M2	0°	Cleaned	
M4	0°	Original	
M5	45°	Original	
M6	45°	Cleaned	

averaged over one single rotation. The use of magnet triggering reveals the possibility of separating the signal correlated to the different orientations of the fibres. The continuous rotations are measured at 2 kHz, and the overall graphs consist of 100 points, corresponding to one measurement for each 100 rounds.

For an in-depth study of the surface features on the wear track, SEM micrographs are used as a *post mortem* research technique. For these studies, small rectangular pieces (40 by 10 mm) were selected over the perimeter of the composite disc including different fibre orientations relative to the sliding direction (Fig. 3). The test specimens were numbered (see Table 2), and the samples with identical fibre orientation were either kept in original form or chemically cleaned with acetone. In that way, the adhering film that has been formed in the wear track under sliding is removed. Because of the well-known fibre orientation, cross-sectional pictures can be taken. Images from the top of the wear track as well as from the cross section of this track, were taken.

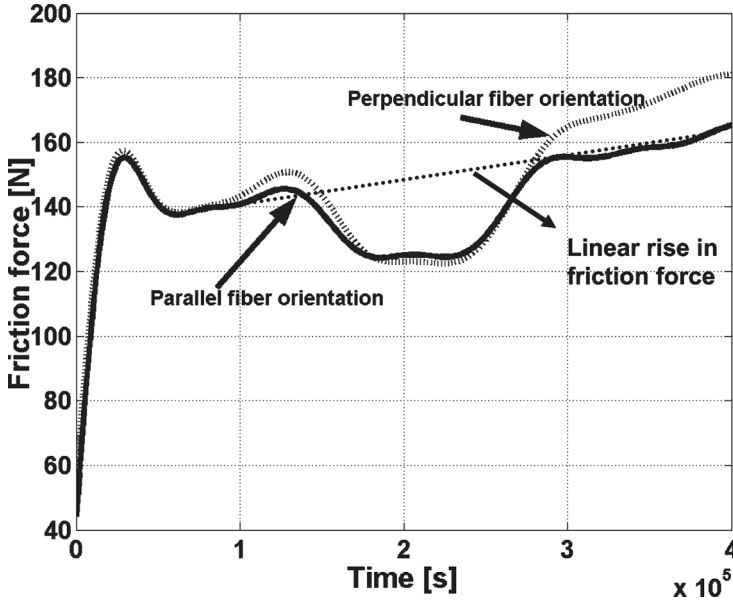
### 3. TEST RESULTS

In this section, the results of friction and wear measurements are shown. Further, the resulting state of the wear track is analyzed for a better understanding of the observed tendencies.

#### 3.1. Frictional Results

##### 3.1.1. Friction Force in Time

A characteristic result of the kinetic friction force as a function of time is presented in Fig. 4. This figure gives the evolution in time (one mean value for each rotation) of the kinetic friction



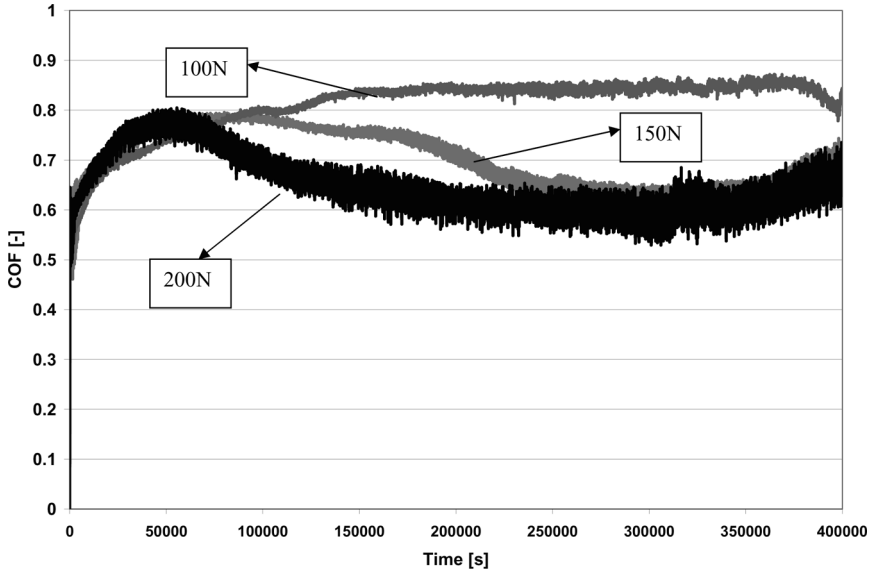
**FIGURE 4** Characteristic result of the friction force as a function of time, related to the fibre orientation within the composite material.

force of the steel–composite pair for a normal load of 250 N and a speed of 10 mm/s. In this graph, there are several regions to be determined.

In the first stage, called the *running-in period* [42–46] of both the pin and the disc, the friction force sharply rises. This might be attributed to a change in surface roughness [42] or to the change in conformity of the contact surfaces during the running-in period [43–46]. After the running-in period (25,000 s), the friction force decreases by 20% (from 150 N to 120 N) after 150,000 s of sliding time. After 270,000 s, the friction force rises again. At 290,000 s, it reaches a value that originates from linear extrapolation of the first friction regime. This final value would occur if widening of the wear track was the only influencing parameter [47]. A lower friction force around 200,000 s, however, points towards intermediate changes in friction mechanism.

### 3.1.2. Influence of Normal Load

In Fig. 5, where the coefficient of friction (the friction force divided by the normal load, in order to scale) is plotted against time, clear load



**FIGURE 5** Evolution of COF with different loads (100 N, 150 N, and 200 N) at a constant velocity of 10 mm/s.

dependence can be seen. At 100 N, the coefficient of friction rises to a steady state value of 0.85. Only near the end of the test is a decrease in COF is measured. Comparing with the friction at 150 N, an identical increase in COF can be seen, but there is a more gradual decrease in COF. Half way, this tendency reaches a steady state value of 0.6. The evolution of the 200-N test indicates the same rise in COF, but a faster lowering of the COF, and a small rise near the end of the test. If this graph is compared with Fig. 4, where the normal load was 250 N, a different behaviour with load can be noticed.

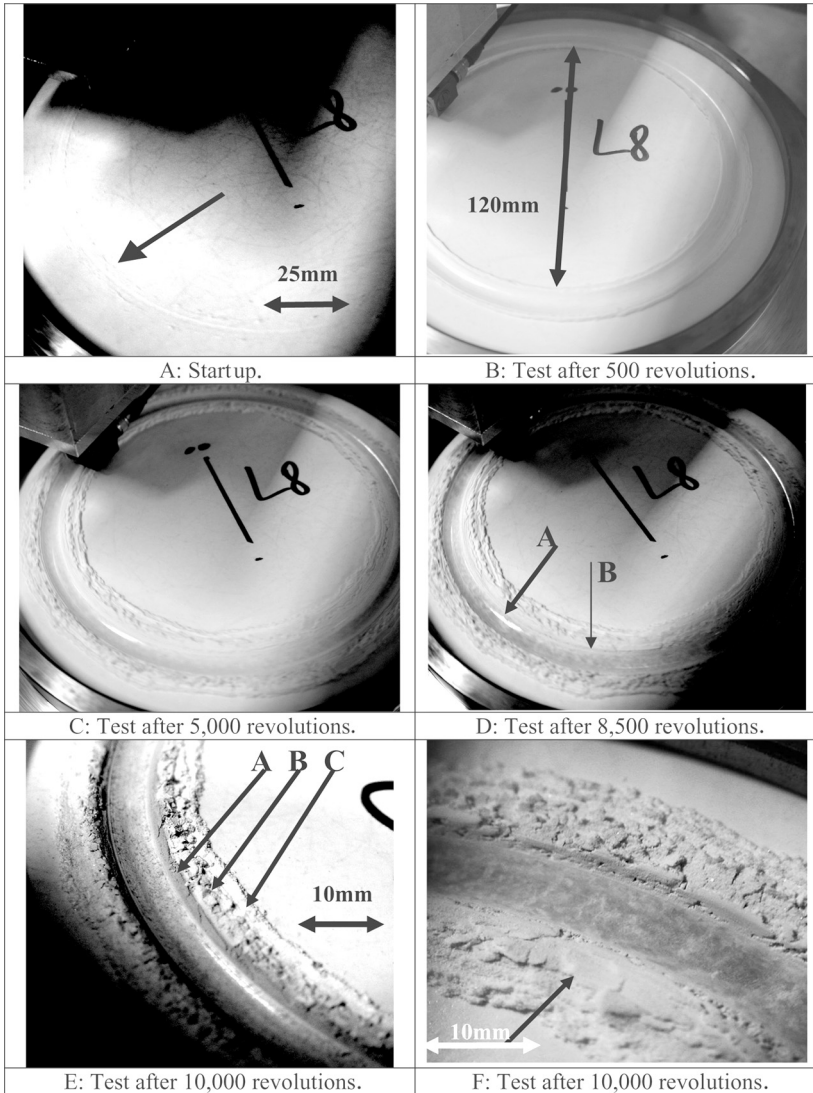
### 3.1.3. Influence of the Orientation of the Fibres

For composite materials, orientation of the fibres plays an important role [5] and, because of the layout of present test setup, differences in frictional behaviour can be easily demonstrated, as shown in Fig. 4. Before the friction force lowers at 150,000 s, there is a small difference in the value of the friction force regarding the fibre orientation. After 290,000 s, a clear separation in the COF with fibre orientation is visible; the parallel orientation has a lower value. This graph, consisting of 100 points for each orientation, gives an indication of the mean value of the coefficient of friction of two corresponding orientations ( $0^\circ$  and  $180^\circ$ ,  $90^\circ$  and  $270^\circ$ ).

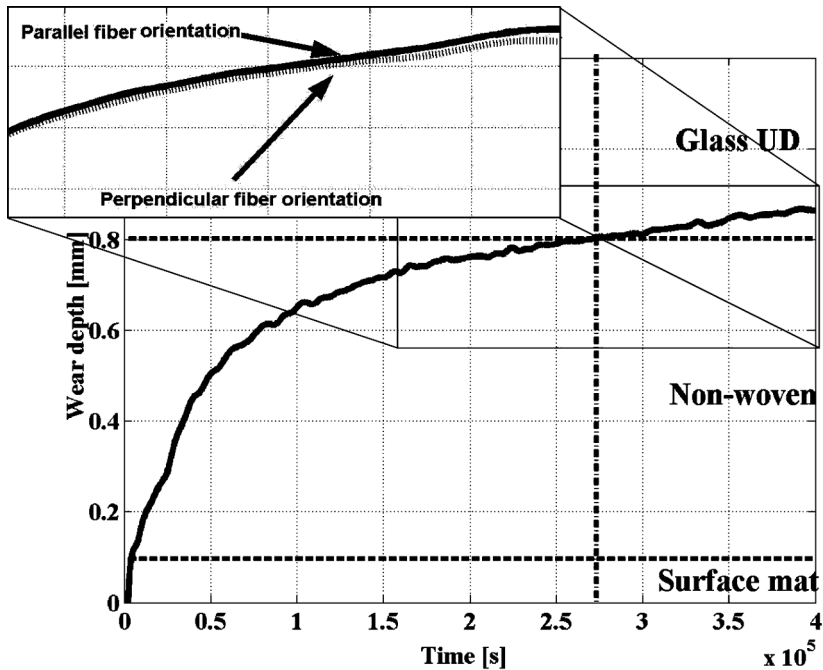
## 3.2. Wear Behaviour in Time

### 3.2.1. Wear Evolution in Time

The evolution of the wear track in time is indicated in Fig. 6 (macroscopic images) and Fig. 7 (measured depth of the wear track). It is



**FIGURE 6** Evolution of wear process in time, with a closer look at particles and their behaviour in time.



**FIGURE 7** Wear-depth evolution in time at 250 N and 10 mm/s, with indication of the structure of the material. A separation with fibre orientation is also shown.

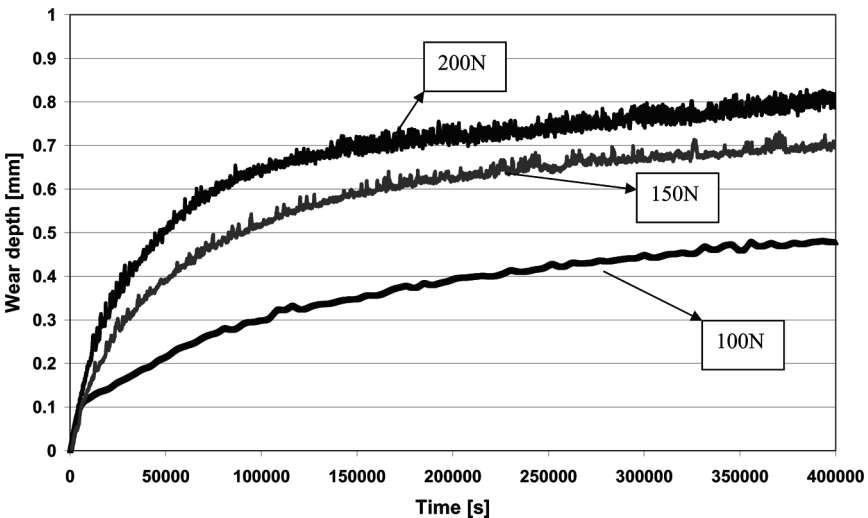
clear from Fig. 6 that the composite material wears relatively more than the steel pin. Immediately after starting the test, a small wear track is formed on the composite disc, as indicated by the arrow in Fig. 6A. Later on, the wear track progressively grows, and disc particles are found near the wear track. In the beginning (Fig. 6B) these particles have the same white colour as the original material. The particles on either side of the wear track can move along the surface of the disc. If seen later during the test, more and more particles accumulate near the wear track. Dark zones (Fig. 6D, arrow B) and a shiny zone (Fig. 6D, arrow A) are visible in the wear track itself. At the end of the test, particles near the wear track have different colours: from the original material colour to nearly black (Fig. 6E, arrows C, B, A). Figure 6F gives an overview of the positioning of the particles after the test. The particles on the outer diameter have lots of free space, and pressed away from the wear track, they give a more open structure. Particles on the inner diameter are pressed together

and, therefore, forced to create agglomerates, yielding to create larger particles at the inner diameter as indicated in Fig. 6F.

The depth of the wear track is measured as a function of time, as shown in Fig. 7. The zones of the material that are worn through, corresponding to the material zones as in Fig. 2 (of course in reversed order), are also indicated on this graph. When wear takes place, the upper layer (the surface mat) needs first to be removed before wear of the deeper regions [nonwoven, unidirectional (UD) fibres] starts. The surface mat is almost immediately worn away (it is only 0.1 mm thick), and afterwards, it takes time to wear through the nonwoven. Finally, the nonwoven is worn away after 290,000 s, and the pin makes contact with the UD-fibre zone (after a depth of 0.8 mm).

### 3.2.2. Influence of Normal Load

The influence of the normal load on the wear depth is given in Fig. 8, showing the evolution of the wear-track depth as a function of time for 100-N, 150-N, and 200-N normal loads. This graph shows that higher loads result in higher wear rates [4,9], meaning a faster rise in wear depth. Also interesting to note is the total wear depth at the end of the test: the UD fibres are slightly touching for the 200-N test, whereas the test fully ends in the nonwoven section under 150-N normal load, and it ends at half the depth of the nonwoven for the



**FIGURE 8** Wear-depth evolution in time for different loads (100 N, 150 N, and 200 N).

100-N test. No UD fibres are worn during the tests under normal loads of less than below 200 N. For a 250-N test, the UD fibre zone was surely attained during wear.

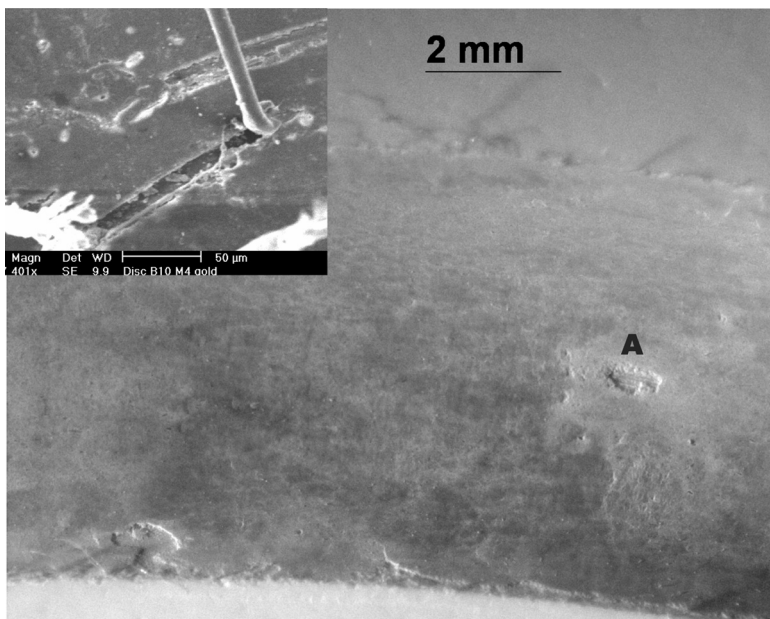
### 3.2.3. Dependence of the Orientation of the Fibres

As indicated in Fig. 7, there is not much difference in the wear comparing different fibre orientations, although the perpendicular orientation gives the lowest wear rate [7]. The material structure (pultruded profile) requires a certain time to wear through the upper layers and finally reach the UD fibre zone. In this case neither the time nor the load were enough to give a clear indication of wear dependence on fibre orientation.

## 3.3. Wear Scar Analysis

### 3.3.1. Wear Scar

A detail of the wear track shown in Fig. 9 by optical microscopy reveals the final state of the worn surface. The inset of the picture, which is part of the outer diameter of the wear track, shows polyester fibres that are part of the surface mat on top of the material (see



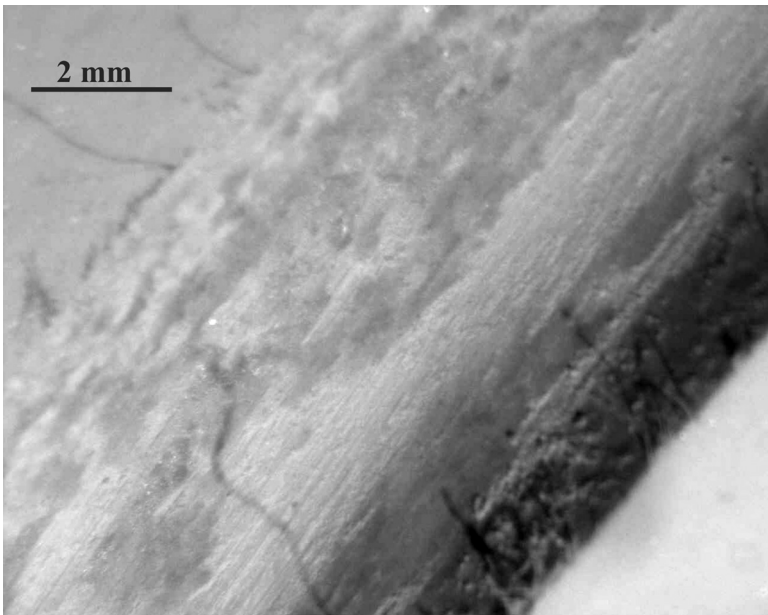
**FIGURE 9** Film on wear track (300 N, 30 mm/s).



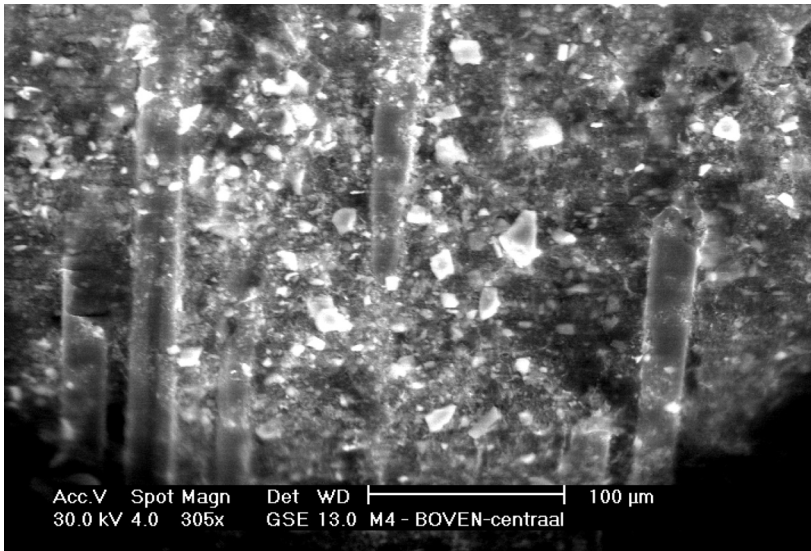
Fig. 2). These fibres did not break, and remain fully attached to the base material after wear. Some of these fibres (see inset) are sometimes pressed or torn away, yielding wear outside the wear track, which is induced by the fibres.

In the wear track itself, a thin film is visible. Holes in this film can be noticed, which make clear the original composite bulk structure (A) underneath. Also a difference in wear damage is detectable, probably due to some temperature effects. This picture was taken after a run for 10,000 cycles at 30 mm/s. If compared with Fig. 10, which gives the final wear track at 250 N and 10 mm/s, a different structure is noticed. At both the inner and the outer diameter, loose fibres are observed, and the film that seemed to be uniform at 30 mm/s is now completely damaged and removed in the middle of the wear track. Near the edges, there are still lots of film fragments (the third body) visible. The underlying structure clearly shows the parallel fibre orientation.

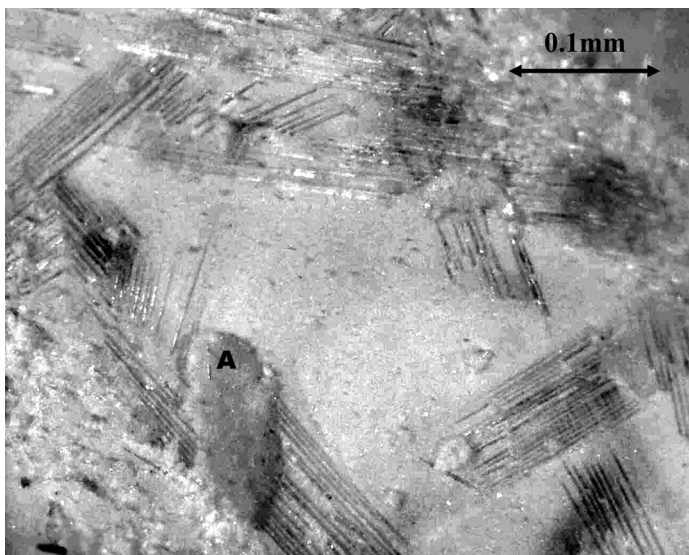
Figure 11 shows a SEM picture at high magnification (305 $\times$ ) of the wear scar as previously shown in Fig. 10, with a clear indication of the fibre orientation. Also, some loose particles (third body) are observed.



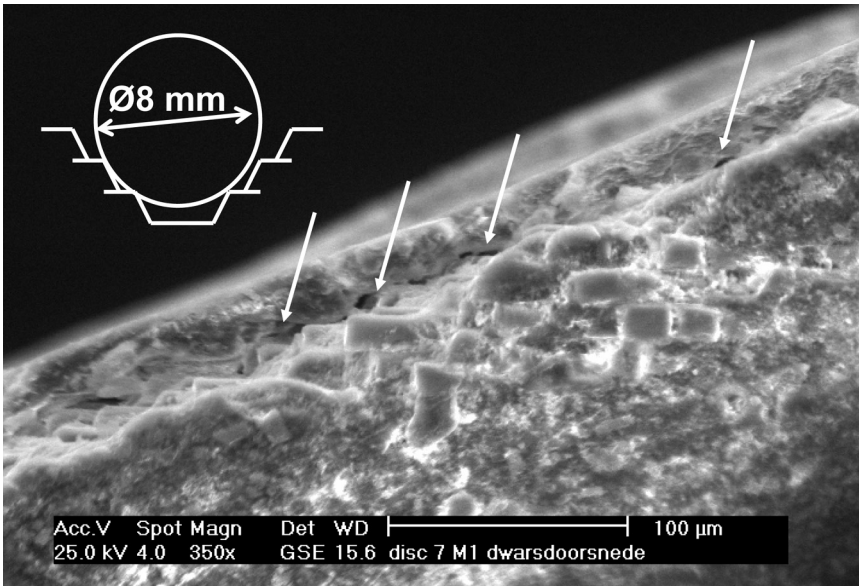
**FIGURE 10** Final wear track at 250 N and 10 mm/s.



**FIGURE 11** Wear track top view, after the test at 250 N, 10 mm/s, and breakthrough of the thin polymer film, parallel fibre orientation.



**FIGURE 12** Damage to the underlying surface after cleaning the wear track with acetone.



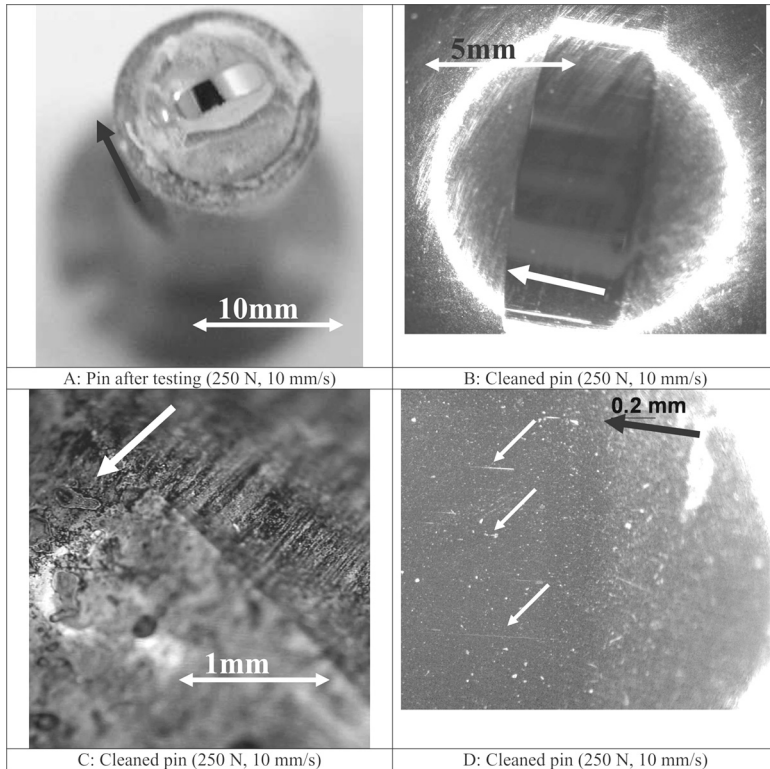
**FIGURE 13** Cross-section of the wear track, with a closer look at the friction transfer film. In the left corner, a schematic cross-section of a wear track is given.

If this thin film is chemically removed with acetone, a subsurface as in Fig. 12 becomes visible. This subsurface reveals a clear view of the fibre bundles of the nonwoven zone. Also, specific wear zones can be seen. Zone A, where a complete bundle of fibres is removed, resulting in a crater, is such a zone. The shiny parts on this picture are polished glass fibres.

A cross-sectional view of the final wear track is shown in Fig. 13. This figure provides insight in the structure of the wear track (see inset) and gives a clear view of the already-mentioned thin film in the wear track. The surface of the film in contact with the pin top is smooth, whereas the surface of the basic material follows a stepwise form. This is due to the fibres, as can be clearly seen in Fig. 13. Beneath the film, there are voids visible, always near glass fibres.

### 3.3.2. Pin

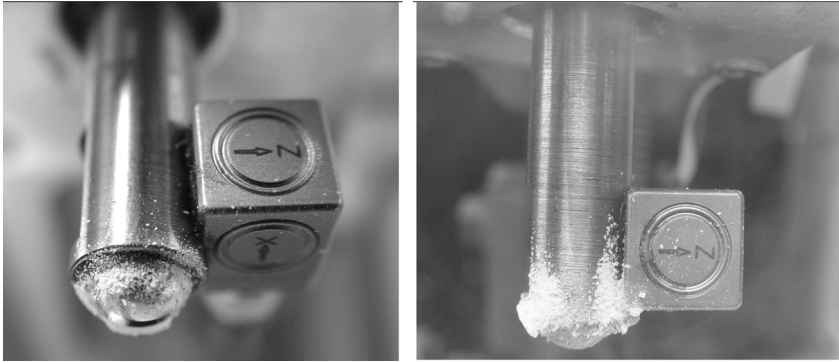
The wear behaviour of the pin is illustrated in Fig. 14. When the pin is removed from the test rig after a sliding distance of 4 km, wear damage as in Fig. 14A (polished elliptical zone) is observed.



**FIGURE 14** Pin after testing, with (A) pin immediately after testing (photo), (B) after cleaning (light microscopic image), (C) outside of the wear track on the pin (metal graphic image), and (D) inside of the wear track on the pin. Arrows indicate each time the disc moved in relation to the pin.

The sliding direction of the disc relative to the pin is indicated by the arrow. This means that particles are only found near the wear track on the pin, on locations where the disc enters the pin (where the particles in the wear track will hit the pin, before being moved aside or taken under the pin, with the front of the pin relative to the rotation of the disc). After cleaning the pin and using optical microscopy, the wear track on the pin looks like Fig. 14B. If this figure is observed in closer detail, two important things can be mentioned:

- First, a straight line occurs at the outside of the wear track (where the disc leaves the pin), as given in Fig. 14C. Also visible are parallel lines in the direction of movement.



**FIGURE 15** Pin after testing: influence of the speed on the particle adhesion to the pin, (A) 10 mm/s and (B) 30 mm/s.

- Second, where the first contact is made between disc and pin under rotation, no straight line can be seen. Figure 14D shows that there is hardly any line, which, together with Fig. 14A, seems reasonable because of the attached particles and the transport of these particles in all directions (under the pin, beside the pin, and higher on the pin). Here, also, parallel lines can be seen in the direction of movement.

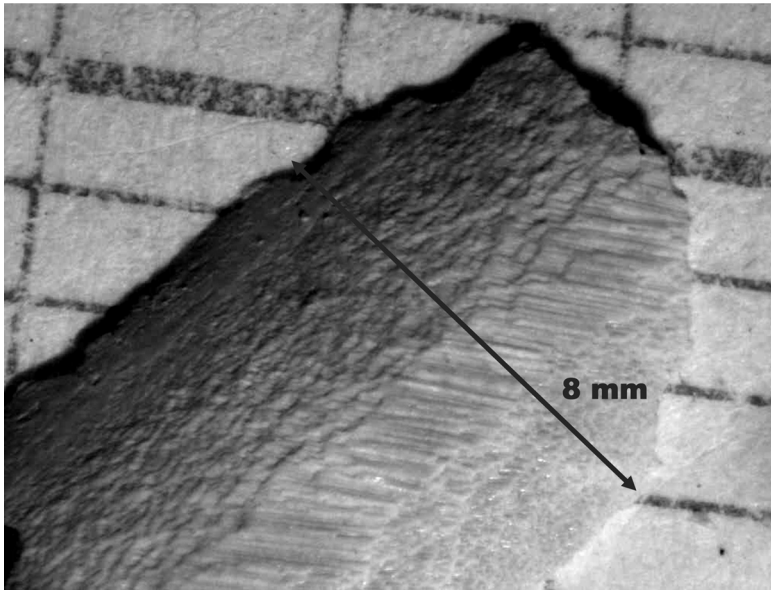
Related to the rotational speed, Fig. 15 shows the pin with adhered wear particles after testing. Lower speeds yield fewer attached particles, whereas with increasing speed, the particles on the pin, parallel with the direction of rotation, adhere more strongly (rise higher) on the pin. The only influencing factor is the rotational speed. This indicates that it might be due to electrostatic loading.

### 3.3.3. Third Body

As wear was observed during testing, wear debris accumulates over the entire disc (see Fig. 6), and its motion or adhesion plays an active role in the total wear and frictional process.

First, debris particles attach to the pin, yielding large differences in the inner and outer zone of the wear track of the pin.

Second, wear particles form a film on the mating surface as can be seen in Figs. 9 and 10. This film then plays the role of third body: it acts as a new body between the composite disc and the steel pin. This third body is built of particles that conglomerate and partially adhere to the original composite surface. A part of this third-body film, after we remove it from the wear track with acetone, is shown in Fig. 16.



**FIGURE 16** Film particle that covered the whole width of the wear track (the left side is the inner diameter of the wear track).

The structure of these film particles consists of parallel layers and, as already mentioned together with Fig. 13, it follows the underlying structure exactly. The layered form of the film particles at the edges and the fibril structure in the centre indicate the fibre orientation of the original polymer composite. A negative representation of the composite fibre structure indicates that particles were squeezed into the composite surface during sliding.

#### 4. DISCUSSION

The results obtained for friction and wear behaviour can be partially related either to changes in composite structure with ongoing wear depth or to the formation of an adhesive film in the wear track.

The relationship of friction and wear to the pultruded material structure can be deduced from Figs. 4 and 7. In both graphs, the evolution in time of the coefficient of friction (Fig. 4) and the wear depth (Fig. 7), which is directly correlated to the material structure (see Fig. 2), are presented. The COF lowers when the surface mat is worn through. Only in the case of 100 N, where a stable high COF is reached and maintained, does this phenomenon not seem to take

place. In the case of 250 N (Fig. 4), a clear difference with different fibre orientations during wear of the UD fibre zone is noticed [5]. This difference is mainly caused by the influence of the fibre orientation relatively to the pin. When the orientation of the fibres is perpendicular to the direction of movement, the pin needs to move across the fibres, yielding a higher friction force. In the case of a parallel orientation, the pin smoothly slides along the fibres and it possibly presses the fibres out of the centre of the wear track for better sliding. This is shown in the insert of Fig. 7, where a much smaller difference in wear depth with fibre orientation can be seen after a difference in friction force depending on the fibre orientation (after 290,000 s). The parallel orientation has a greater depth than the perpendicular orientation, as a result of the possible movement of the parallel fibres with the pin. The difference in the COF with fibre orientation proves that the main contact between pin and disc is still in the middle of the wear track, although a large wear scar can be seen on the pin after testing. It is assumed that the latter edges do not bear much of the normal load, although they have to wear to widen the wear track with increasing wear depth. The rise in the beginning of the test, where the friction force rises in 20,000 s with more than 100 N (Fig. 4), can easily be explained by taking into account the running-in effect of pin and disc, where the contact area between both sliding bodies rises (a point over the line to an elliptical contact), and also the ploughing component of the COF rises. The drop in friction force results because after reaching a maximum, the main load is transferred to the top of the pin, in the middle of the wear track, where the contact is more rigid (because of the glass fibres) and the ploughing component of the friction force lowers. In the case of 250 N, an extrapolated linear rise of the friction force is attained after intermediate lower friction. This gives an indication that the lowering with 20% of the friction force around halfway through the test is a result of something that disappears again, at this speed.

As seen in other different tests, and in some tests of shorter duration, a thin film is formed, not on the pin but on the wear track (Figs. 9, 10, and 12). Because the formation of this film is related to the applied normal load, sliding velocity, and the material's structure, only conclusions for low-speed sliding can be drawn (Fig. 9). Because of this film, the rise in friction under a 250-N normal load can be explained by the theory of Finkin [48], giving an explanation of the phenomenon of increasing friction with a progressive decrease in the film thickness. The film in this test really decreases and is finally removed, which can be concluded from the SEM picture (Fig. 11) and the macro in Fig. 10. The rise in friction force and its relation to

the original fibre orientation proves that the film finally has disappeared after 270,000 s of sliding. The breakthrough, as seen in Fig. 10, only takes place in the centre of the wear track, which proves again that the load-bearing capacity is only located in the centre of the wear track and that the edges do not bear any of the applied load. A decrease in film thickness is partially the result of the low speed in combination with the more rigid structure of the UD fibres.

As mentioned before, the normal load is only carried in the centre of the wear track, although if the wear track progressively grows, the edges also need to wear. This is not due to the normal load. Other possibilities for the wear of the edges are the frictional force (ploughing component of friction) and the movement of particles from the centre of the wear track to the edges, where they act as abrasive particles.

The frictional component certainly plays a role, although we need to take into account the film in the wear track. This results in a combined mechanism. The friction force not only influences the wear of the edges but also influences the film. This film is built up of layers (Fig. 16) that can move over each other and is called a *solid lubricating* film. This immediately explains the lower friction force as seen in Fig. 4.

There are several mechanisms that play an important role in the formation of this thin film, mainly resulting from re-adhesion of wear debris. This wear debris comes from different sources: particles from the edge, particles attached to the pin (electrostatic attraction), and material removed from the subsurface, and is mainly determined by the linear speed [13,29,30] and the material structure.

First, related to the wear in time of these composites, a change in the width of the wear track causes the particles to be pressed to the side of the wear track, as shown in Fig. 6. When the wear track grows (becomes wider and also deeper), the particles are forced by the pin to move aside on the top of the original disc surface, or they will be pressed under the pin. Looking at the final result of the disc validates this statement. Wear particles, with different shades (from pure white to nearly black), can be found on both sides of the wear track, with the white ones the farthest from the track as a result of the earliest removal and being pushed aside by new wear particles. The change in shade of the particles is due to (normal) contact forces in the centre of the wear track, the speed, and, as a result of both, also the temperature. These darker particles all were once part of the thin film. Looking at Fig. 13, a cross-sectional view of the wear track, voids can be seen under the film, strongly related to visible fibres. This points out that after testing, although the film strongly adheres to the wear track, the strong bonds are created between the film and the matrix material, and the adhesion of the film to the glass fibres hardly exists.



This film is build up from wear debris either adhering to the steel pin or falling down from the edges of the wear scar. The latter mechanism is the least important, because of rotation of the disc and particles that lost contact with the pin on the outside of the pin. As shown in Fig. 15A and B, particles are attached to the outside of the pin. Because of the rotation of the disc, the pin is electrostatically loaded, and particles are attracted to the pin. The electrostatic loading only starts when the first glass fibres are visible; this is after the removal or wearing through of the top surface layer. When those particles start moving upwards on the pin, there will be a position where the attractive forces are too low to keep these particle agglomerates sticking to the pin, and large agglomerates of single particles lose contact and fall into the composite wear track, hitting the pin, each time at the same side after one rotation as shown in Fig. 14A.

A third possibility is fresh debris that originates from the sub-surface takes part in the film formation, as confirmed by an optical microscopic image (Fig. 12) when the polymer film is removed with acetone and the original composite structure (substructure) is visible. This picture shows the wear process in the centre of the wear track. The damage (matrix removal) visible on this surface is purely due to the test and not to the method of removing the film. In this picture, after a wear test (60 N, 10 mm/s), fibre bundles of the nonwoven are clearly visible. The region marked A is a region where fibres are broken down and removed, indicating that during the formation, deformation, and/or removal of the thin polymer film, not only are particles from the edges are pressed into the film but also material from beneath the film is used to build up this polymer film. This image is a view of the nonwoven (bundles of fibres).

These three mechanisms result in a thin transfer film in the composite wear track.

Once the film is established, the ongoing pressure of the pin and wear lead to possible deformation of this film, mainly when the UD fibres start to wear (see the result in Fig. 10). This deformation is strongly related to the sliding velocity of the test. For higher velocities (Fig. 9, 30 mm/s), hardly any destruction and removal can be seen. At a lower sliding speed (10 mm/s), the transfer film is seen during initial wear of the non-woven structure but disappears when the UD fibres are worn. Thus, a second parameter influencing film deformation is the structure of the material. In the bulk of the present pultruded composite, there are UD fibres, which indicate a better and closer position of the fibres related to each other. Therefore, less matrix material is available and a stiffer structure is attained. At low speeds, the film deforms, and is almost completely removed in the centre of the

wear track (Fig. 10). When a higher speed is provided, even when the UD fibres are reached, a thin film at the wear track still remains. A possible explanation for this phenomenon is the influence of the temperature on the film formation [30], and in more detail, the temperature as a result of the higher speed.

Because of the rotation of the disc with respect to the pin, the film is built up and the movement of the particles throughout the film can be seen in Fig. 13.

Wear mechanisms as found in the literature [2,37–41] are also observed in these tests. The typical wear mechanisms of polymer matrix composites are fibre breaking, fibre-matrix debonding, and matrix fracture. Other important mechanisms are fibre pullout, matrix wear related to fibre movement, peeling of the matrix, shear deformation of the fibres, and deformation of the edges of the wear track. As a result of the thin transfer film, the sliding behaviour of the pin-disc configuration is transformed into a shear-based behaviour. The pin only provides the normal load, which, as a result of the rotation of the disc, is within the transfer film transformed into shear. Because of the geometrical setup, this shear is not only in the direction of movement (friction film) but also perpendicular to the direction of movement and results in particles being pressed out of the wear track (Fig. 13) and put aside on the top surface of the disc.

The nonwoven structure itself strongly influences the edges of the wear track. Although with pure polymers, a smooth continuous edge of the wear track can be expected, this is not the case with polymer matrix composites. The edges take irregular forms related to the orientation of the fibres. This results in removal of parts of the matrix material, parallel to the fibre orientation at that particular place, independent of the fibre orientation related to the direction of motion. Also, inside the wear track (cross-section), a stepwise formation (Fig. 13) in depth is seen, but a view from above also shows that in the horizontal plane no smooth lines can be seen. Here the wear track follows the fibres, which break at their weakest point or in fatigue, and the step form is only dependent on the fibres. As a result of particles being pressed out of the wear track, near the edges, the wear track is wider than would be expected and has no perfectly round cross section. Instead of following the form of the pin (ball or slightly worn ball), more material is removed near the edges. This is the result of the shear forces acting perpendicular to the direction of movement. As mentioned before, the thin transfer film is pressed out of the wear track during testing. This happens as fast as a new one can be formed. Because of the movement of these particles, wear is induced near the edges, which results in a wider track at the original surface (third-body abrasion) [28–29].

## 5. CONCLUSIONS

The following conclusions can be drawn from this investigation:

1. The frictional behaviour is influenced by many parameters, but most pronounced is the formation of a thin film. This film yields a reduction in friction force of 20%. At low speeds (10 mm/s), the material structure plays the most important role in frictional behaviour, whereas at higher speeds (30–40 mm/s) the film is more continuous, resulting in a more stable coefficient of friction. Once the UD fibres are reached, they also influence the frictional behaviour. Parallel orientation results in a lower coefficient of friction compared with the perpendicular orientation.
2. Three main mechanisms of film formation are indicated:
  - a. particles falling from the edges into the wear track;
  - b. particles attached to the pin;
    - i. particles hitting the pin above the film, on the outside;
    - ii. particles attached to the pin as a result of electrostatic forces;
  - c. material from the underlying surface.
3. The influence of this re-adhesion on the wear is difficult to understand. The re-adhesion does not influence the known wear mechanisms. The shear forces in pure pin–disc contact seem to be transformed to shear forces within the film, yielding the same wear mechanisms but with a reduction in wear rate. However, the abrasive action of film particles pressed out of the wear track results in a new wear mechanism, abrasive wear, perpendicular to the direction of movement.

## ACKNOWLEDGEMENTS

This work was financially supported by the BOF (special research fund) of Ghent University, Belgium. The authors acknowledge the assistance of W. Van Daele for the help taking SEM pictures and R. Desmet and C. Vermeulen for help with the technical development of the test rig, test samples, and constant advice.

## REFERENCES

- [1] Henry, S. D., *Materials for Friction and Wear Applications*, ASM Handbook, (ASM International, Materials Park, Pa., 1992).
- [2] Ramesh, R., Kishore, K. K., and Rao, R. M. V. G. K., *Wear* **89**, 131–136 (1983).
- [3] Biswas, S. K. and Vijayan, K., *Wear* **158**, 193–211 (1992).

- [4] Friedrich, K., (ed.), *Friction and Wear of Polymer Composites*, Composite Materials Series (Elsevier, Amsterdam, 1986), Vol. 1, p. 233.
- [5] Jacobs, O., Friedrich, K., Marom, G., Schulte, K., and Wagner, H. D., *Wear* **135**, 207–216 (1990).
- [6] Khedkar, J., Negulescu, I., and Meletis, E. I., *Wear* **252**, 361–369 (2002).
- [7] Tripathy, B. S. and Furey, M. J., *Wear* **162–164**, 385–396 (1993).
- [8] Lu, Z. P. and Friedrich, K., *Wear* **181–183**, 624–631 (1995).
- [9] Friedrich, K., Karger-Kocsis, J., and Lu, Z. P., *Wear* **148**, 235–247 (1991).
- [10] Cirino, M., Pipes, R. B., and Friedrich, K., *J. Mater. Sci.* **22**, 2481–2492 (1987).
- [11] Bijwe, J., Logani, C. M., and Tewari, U. S., *Wear* **138**, 77–92 (1990).
- [12] Bijwe, J., Indumathi, J., Rajesh, J. J., and Fahim, M., *Wear* **249**, 715–726 (2001).
- [13] Filip, P., Weiss, Z., and Rafaja, D., *Wear* **252**, 189–198 (2002).
- [14] Rhee, S. H. and Ludema, K. C., *Wear* **46**, 231–240 (1978).
- [15] Wirth, A., Eggleston, D., and Whitaker, R., *Wear* **179**, 75–81 (1994).
- [16] Wahl, K. J. and Singer, I. L., *Tribol. Lett.* **1**, 59–64 (1995).
- [17] Schön, J., *Wear* **257**, 395–407 (2004).
- [18] Cowan, R. S. and Winer, W. O., *Proc. Leeds-Lyon 1989: Thin Films in Tribology*.
- [19] Wang, Q.-H., Xue, Q.-J., Liu, W.-M., and Chen, J.-M., *Wear* **243**, 140–146 (2000).
- [20] Lancaster, J. K., *Tribology* **6**, 219–251 (1973).
- [21] Briscoe, B. J. and Tabor, D., *Fundamentals of Tribology* (Suh and Saka, Cambridge, 1980), pp. 733–758.
- [22] Yust, C. S., Leitnaker J. M., and Devore, C. E., *Wear* **122**, 151–164 (1988).
- [23] Rigney, D. A., Chen, L. H., Tayler, M. A. S., and Rosenfield, A. R., *Wear* **100**, 195–219 (1984).
- [24] Stott, F. H. and Wood, G. C., *Tribol. Int.* **11**, 211–218 (1978).
- [25] Jacko, M. G., Tsang, P. H. S., and Rhee, S. K., *Proc. Int. Conf. on Wear of Materials* (ASME, New York, 1989), pp. 469–479.
- [26] Godet, M., *Wear* **100**, 437–452 (1984).
- [27] Berthier, Y., Godet, M., and Brendle, M., *Tribol. Trans.* **32**, 490–496 (1989).
- [28] Godet, M., *Wear* **136**, 29–45 (1990).
- [29] Sviridenok, A. I., *Soviet Journal of Friction and Wear* **8**, 773–778 (1987).
- [30] Hawthorne, H. M., *Wear* **149**, 169–185 (1991).
- [31] Kishore, Sampathkumaran, P., Seetharamu, S., Murali, A., and Kumar R. K., *Wear* **247**, 208–213 (2001).
- [32] Quintelier, J., De Baets, P., Degrieck, J., De Geyter, M., and Philips W., *Proc. 8th International Conference on Tribology*, 2004, pp. 36–42.
- [33] Davim, J. P. and Marques, N., *Journal of Materials Processing Technology* **152**, 389–394 (2004).
- [34] Friedrich, K., Flöck, J., Váradi, K., and Néder, Z., *Wear* **251**, 1202–1212 (2001).
- [35] Fusaro, R. L., *Lubr. Eng.* **42**, 668–676 (1986).
- [36] Pödra, P. and Andersson, S., *Trib. Int.* **32**, 71–81 (1999).
- [37] Vangrimde, B. and Boukhili, R., *Composite Structures* **58**, 57–73 (2002).
- [38] Chand, N., Naik, A., and Neogi, S., *Wear* **242**, 38–46 (2002).
- [39] El-Tayeb, N. S. M. and Mostafa, I. M., *Wear* **195**, 186–191 (1996).
- [40] El-Tayeb, N. S. and Gadelrab, R. M., *Wear* **192**, 112–117 (1996).
- [41] Pihtili, H. and Tosun, N., *Compos. Sci. Tech* **62**, 367–370 (2002).
- [42] Pawlus, P., *Wear* **176**, 323–334 (1991).
- [43] Wang, F., Lacey, P., Gates, R. S., and Hsu, S. M., *J. Tribol. Trans.* **113**, 755–761 (1991).
- [44] Tyagi, M. R. and Sethuramiah, A., *Wear* **197**, 89–97 (1996).

- [45] Tyagi, M. R. and Sethuramiah, A., *Wear* **197**, 98–104 (1996).
- [46] Wu, C. W. and Zheng, L. Q., *Wear* **147**, 323–334 (1991).
- [47] Bowden, F. P. and Tabor, D., *The Friction and Lubrication of Solids* (Oxford University Press, Oxford, UK, 1964), Pt. II pp. 114–117.
- [48] Finkin, E. F., *J. Lubric. Technol.* **91**, 551–556 (1969).